 CMES, vol.63, no.1, pp.29-45, 2010

Finite Element Nonlinear Analysis for Catenary Structure Considering Elastic Deformation

B.W. Kim[1], H.G. Sung[1], S.Y. Hong[1] and H.J. Jung[2]

Abstract: This paper numerically investigates the behavior of sag and tension of inclined catenary structure considering elastic deformation. Equilibrium equation for computing elastic catenary is formulated by employing finite element method (FEM). Minimum potential energy principle and the Lagrange multiplier method are used in the formulation to derive equilibrium equation with constraint condition for catenary length. Since stiffness and loading forces of catenary are dependent on its own geometry, the equilibrium equation is nonlinear. Using the iterative scheme such as fixed point iteration or bisection, equilibrium position and tension are found. Based on the formulation, a Fortran solver is developed in this study. With the solver, numerical analyses for example catenary structures are carried out. From the numerical examples, the sag and tension of catenary only which ignores elastic deformation are compared with those of elastic catenary of which elastic deformation is considered. By analyzing elastic catenary for various axial stiffness conditions, the asymptotic behaviors of sag and tension are examined. Inclined catenary structures with various slopes are also analyzed to study the effect of catenary slope on sag and tension.

Keywords: Catenary, Elastic deformation, FEM, Length constraint, Sag, Tension, Catenary slope.

1 Introduction

Catenary structures are widely used for various engineering applications. Cable of suspension bridge, bracing guy and mooring line for floating body are typical examples of catenary. Analytical and numerical methods for analyzing catenary were presented by many researchers. Huge theories for analytic approach were established by Irvine [Irvine (1981)]. FEM for cable analysis was presented by Bathe [Bathe (1996)]. Numerical schemes were developed for mooring analysis

[1] KORDI/MOERI, Daejeon, Korea
[2] KAIST, Daejeon, Korea

and they are applied in the field of ocean engineering [Hong and Hong (1997); Garrett (2005)].

The equilibrium position of catenary is determined when the external forces and tension are balanced. And, additional stretch is ignored if elongation due to tension is small compared to total length of catenary. This is the case of pure catenary. However, in a exact manner, catenary suffers elastic deformation due to tension and the sag or tension of such elastic catenary will be quite different from those of pure catenary if the material is flexible.

The purpose of this paper is to rigorously investigate the sag and tension of catenary structure including the effect of elastic deformation due to tension and compare the results with the case of pure catenary. Since the equilibrium position of catenary is determined by tension and tension varies with geometry, position and tension of catenary are interactive. The forces acting on catenary are also dependent on geometry. Therefore, the behavior of catenary is geometrically nonlinear. Very flexible beams or shells are also geometrically nonlinear structures. Okamoto and Omura (2003) employed FEM to solve nonlinear beam problems and they showed that the numerical results agree well with experiments. FEM was also successfully applied to nonlinear plate and shell problems [Cui et al. (2008)].

In this study, FEM is employed to numerically analyze the behavior of elastic catenary and a Fortran solver is developed based on FEM. In the FEM formulation, minimum potential energy principle is applied to derive nonlinear equilibrium equation. Constraint equation describing catenary length with elastic stretch is added to potential energy formulation with the use of Lagrange multiplier method. To get the solution of nonlinear equilibrium equation, iterative techniques such as fixed point iteration or bisection are used. By analyzing example catenary structures, the developed solver is verified and the variation of sag and tension of elastic catenary is examined for various values of axial stiffness. Those results are also compared with cases of catenary only. By summarizing the results, the asymptotic behavior of sag and tension is observed. In addition to the elasticity, the effect of installation slope is also investigated by analyzing elastic catenary with various slope angles.

2 Finite element formulation

Geometric configuration of elastic catenary with FEM model is shown in Fig. 1. In the figure, circular points represent nodes and lines between nodes are two-node elements. If total given length of unstretched catenary is s_t, unstretched length of element s_0 can be set as $s_t = \sum s_0$ according to user-defined mesh system. If given gravity force per unit length in unstretched element is w_0, gravity force per unit length in stretched element will be $w = w_0 s_0/s$ where s is stretched length of

element. Then, total gravity force is $W = \sum w_0 s_0 = \sum ws$.

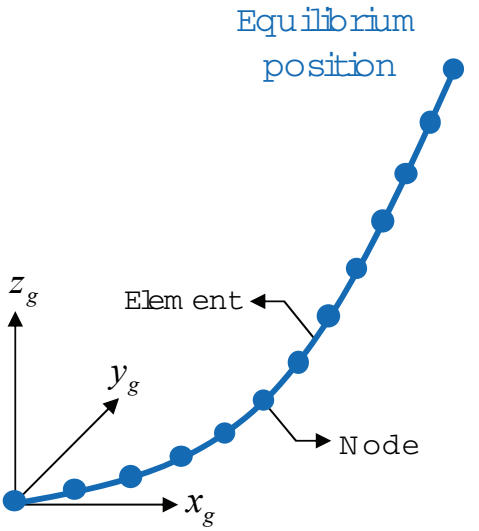

Figure 1: FEM model for elastic catenary

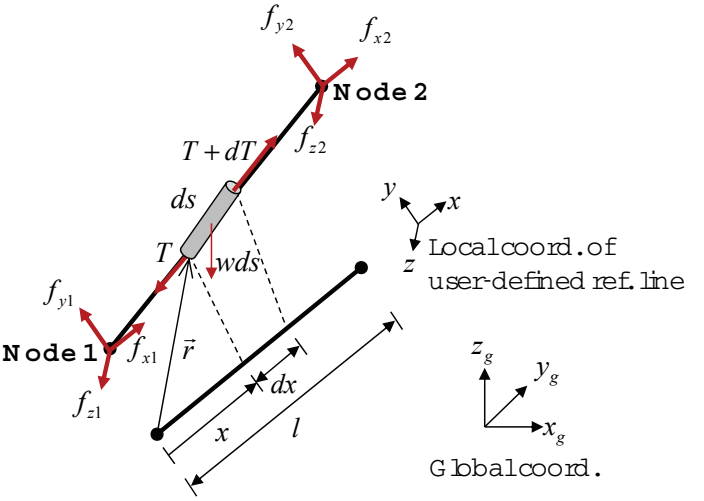

Figure 2: Free body diagram of element

Fig. 2 shows conceptual sketch of free body condition of one element. In the figure,

T is tension at x of local coordinate. The local coordinate is determined from the reference line of user-defined starting mesh system. The reference line closer to solution position will lead to less iteration in numerical computation. l is element length in such reference line. $\vec{r}$ is position vector by local directional displacements u_x, u_y and $u_z$at x. It will take the form

$$\vec{r} = (x + u_x, u_y, u_z) \tag{1}$$

Then, Jacobian J will be

$$J = \frac{ds}{dx} = \frac{|d\vec{r}|}{dx} = \sqrt{(1 + u'_x)^2 + u'^2_y + u'^2_z} \tag{2}$$

Nodal displacements and section forces in local coordinate can be arranged in vector form as

$$\{u_e\} = [u_{x1}\, u_{y1}\, u_{z1}\, u_{x2}\, u_{y2}\, u_{z2}]^T \tag{3}$$

$$\{f_e\} = [f_{x1}\, f_{y1}\, f_{z1}\, f_{x2}\, f_{y2}\, f_{z2}]^T \tag{4}$$

And, they can be transformed to global coordinates as Eqs. 5 and 6 using orthogonal transformation matrix $[T]$ such that $[T]^T[T] = [I]$.

$$\{u_e\} = [T]\{u_{ge}\} \tag{5}$$

$$\{f_e\} = [T]\{f_{ge}\} \tag{6}$$

Since the direction of gravity force is $-z_g$ in global coordinate, work by gravity force takes the following form

$$\pi_w = -\int_s u_{zg} w ds = -\int_0^l u_{zg} w \frac{ds}{dx} dx = -\int_0^l u_{zg} J w dx \tag{7}$$

where u_{zg} is the z_g directional displacement at x and it can be interpolated with nodal displacements as

$$u_{zg} = \left(1 - \frac{x}{l}\right) u_{z1g} + \frac{x}{l} u_{z2g} \tag{8}$$

By inserting it into Eq. 7, arranging it in vector form, integrating it and using coordinate transform as Eq.5, the work will be

$$\pi_w = -\{u_{ge}\}^T \{f_{we}\} = -\{u_e\}^T [T]\{f_{we}\} \tag{9}$$

where

$$\{f_{we}\} = \frac{Jwl}{2}[0\,0\,1\,0\,0\,1]^T \tag{10}$$

Work by section forces is

$$\pi_e = \{u_e\}^T\{f_e\} \tag{11}$$

Constraint equation for length condition is

$$\int_s (ds - dx) = s - l \tag{12}$$

Where s is element length in equilibrium position and it will be Eq. 13 if pure catenary is considered.

$$s = s_0 \tag{13}$$

If the effect of elastic deformation as well as catenary behavior is considered, the length will be

$$s = s_0\left(1 + \frac{T}{EA}\right) \tag{14}$$

where EA is axial stiffness. Energy equation for Eq. 12 can be formulated as Eq.15 using Lagrange multiplier λ.

$$\begin{aligned}
\pi_c &= \int_0^l \lambda\left(\frac{ds-dx}{dx} - \frac{s-l}{l}\right)dx \\
&= \int_0^l \lambda\left(J - 1 - \frac{s-l}{l}\right)dx \\
&= \int_0^l \lambda\left(\frac{J^2-1}{J+1} - \frac{s-l}{l}\right)dx \\
&= \int_0^l \lambda\left(\frac{2u'_x + u'^2_x + u'^2_y + u'^2_z}{J+1} - \frac{s-l}{l}\right)dx
\end{aligned} \tag{15}$$

Interpolating u_x, u_y, u_z with nodal displacements, arranging in matrix form and integrating will lead to the following form

$$\pi_c = \lambda(\{u_e\}^T\{A\} + \{u_e\}^T[C]\{u_e\} - (s-l)) \tag{16}$$

where

$$\{A\} = \frac{2}{J+1}[-100100]^T \tag{17}$$

$$[C] = \frac{1}{(J+1)l}\begin{bmatrix} 1 & 0 & 0 & -1 & 0 & 0 \\ & 1 & 0 & 0 & -1 & 0 \\ & & 1 & 0 & 0 & -1 \\ & & & 1 & 0 & 0 \\ S & y & m & m & 1 & 0 \\ & & & & & 1 \end{bmatrix} \tag{18}$$

By combining Eqs. 9, 11 and 16, total potential energy will be derived as

$$\begin{aligned} \pi &= -\pi_w - \pi_e + \pi_c \\ &= \{u_e\}^T[T]\{f_{we}\} - \{u_e\}^T\{f_e\} \\ &\quad + \lambda(\{u_e\}^T\{A\} + \{u_e\}^T[C]\{u_e\} - (s-l)) \end{aligned} \tag{19}$$

Applying minimum potential energy principle that is $\delta\pi = 0$, we get a set of Lagrange equations as

$$\frac{\partial \pi}{\partial \{u_e\}} = 0 \tag{20}$$

$$\frac{\partial \pi}{\partial \lambda} = 0 \tag{21}$$

By inserting Eq. 19 into Eq. 20, we get

$$\begin{aligned} \frac{\partial \pi}{\partial \{u_e\}} &= [T]\{f_{we}\} - \{f_e\} + \lambda(\{A\} + 2[C]\{u_e\}) \\ &= \lambda[C]\{u_e\} + [T]\{f_{we}\} - \{f_e\} + \lambda(\{A\} + [C]\{u_e\}) \\ &= [K_e]\{u_e\} + [T]\{f_{we}\} - \{f_e\} + \{B\}\lambda \\ &= 0 \end{aligned} \tag{22}$$

where

$$[K_e] = \lambda[C] \tag{23}$$

$$\{B\} = \{A\} + [C]\{u_e\} \tag{24}$$

Eqs. 19 and 21 lead to

$$\begin{aligned}\frac{\partial \pi}{\partial \lambda} &= \{u_e\}^T\{A\} + \{u_e\}^T[C]\{u_e\} - (s-l) \\ &= \{B\}^T\{u_e\} - (s-l) \\ &= 0\end{aligned} \tag{25}$$

Therefore, we get the following equilibrium equations of element in local coordinate.

$$[K_e]\{u_e\} + \{B\}\lambda = -[T]\{f_{we}\} + \{f_e\} \tag{26}$$

$$\{B\}^T\{u_e\} = s - l \tag{27}$$

By coordinate transform, we get equilibrium equations of element in global coordinate as

$$[K_{ge}]\{u_{ge}\} + \{B_g\}\lambda = -\{f_{we}\} + \{f_{ge}\} \tag{28}$$

$$\{B_g\}^T\{u_{ge}\} = s - l \tag{29}$$

where

$$[K_{ge}] = [T]^T[K_e][T] \tag{30}$$

$$\{B_g\} = [T]^T\{B\} \tag{31}$$

$$\{f_{ge}\} = [T]^T\{f_e\} \tag{32}$$

Eqs. 28 and 29 can be rearranged in state space form as

$$\begin{bmatrix} [K_{ge}] & \{B_g\} \\ \{B_g\}^T & 0 \end{bmatrix} \begin{Bmatrix} \{u_{ge}\} \\ \lambda \end{Bmatrix} = \begin{Bmatrix} -\{f_{we}\} + \{f_{ge}\} \\ s - l \end{Bmatrix} \tag{33}$$

Element-by-element combination will lead to the final equilibrium equation for total system as

$$[K]\{u\} = \{f_n\} + \{f\} \tag{34}$$

where

$$[K] = \sum_e \begin{bmatrix} [K_{ge}] & \{B_g\} \\ \{B_g\}^T & 0 \end{bmatrix} \tag{35}$$

$$\{f_n\} = \sum_e \begin{Bmatrix} -\{f_{we}\} \\ s-l \end{Bmatrix} \tag{36}$$

$\{f\}$ is external forces vector acting at nodes. Eq. 35 is stiffness matrix which symmetric and banded. Eq.36 is force vector due to gravity and constraint.

A Fortran program to solve catenary equation is developed in this study based on the procedure as is described above. Since the stiffness matrix and force vector are functions of Jacobian, Lagrange multiplier and displacements, the equilibrium equation is geometrically nonlinear. Iterative scheme such as bisection or fixed point iteration is used to find the nonlinear solution. Once the solution is found, the section forces can be recovered by inserting the solutions into element equation as

$$\{f_{ge}\} = [K_{ge}]\{u_{ge}\} + \{B_g\}\{\lambda\} + \{f_{we}\} \tag{37}$$

Catenary tension is obtained by projecting the section forces to longitudinal line in equilibrium position.

3 Numerical examples

Geometry and particulars of example catenary structure for numerical analysis are summarized in Fig. 3 and Table 1. In the figure, f is the final sag in equilibrium position. Total unstretched length of catenary is 1,026 m and unit gravity is 2,000 N/m resulting in total gravity of 2,052,000 N. Various values for EA are considered in numerical analysis to investigate the effect of elastic deformation and to compare with pure catenary behavior. The effect of slope angles are also observed by analyzing catenaries with θ of 0$\sim$75 deg. In the present study, the following non-dimensional parameters are defined and used for comparative study.

$$EA_n = \frac{EA}{W} \tag{38}$$

$$f_n = \frac{f_{\max}}{L} \tag{39}$$

$$T_n = \frac{T_{\max}}{W} \tag{40}$$

They are non-dimensional axial stiffness, sag, tension, respectively.

In order to validate the developed code, analytic and FEM solutions are compared. In the case of pure catenary, analytic solutions for equilibrium position and tension can be derived as [Arbabi (1991)].

$$z(x) = \frac{H}{w}\cosh\left\{\frac{w}{H}(x_s - x)\right\} - \frac{H}{w}\cosh\frac{wx_s}{H} \tag{41}$$

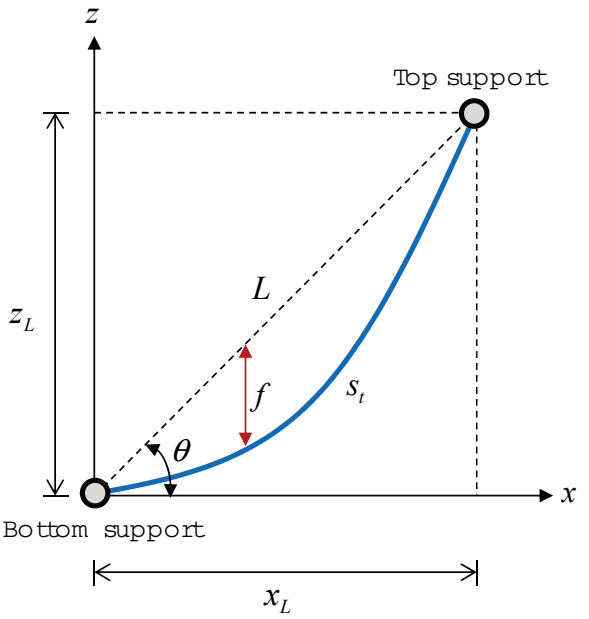

Figure 3: Layout of example catenary structure

Table 1: Main particulars of example catenary structure

Distance between supports (L)	1,000 m
Total unstretched length (s_t)	1,026 m
Gravity per unit length (w_0)	2,000 N/m
Total gravity (W)	2,052,000 N
Non-dimensional axial stiffness (EA_n)	0.3∼3,000
Slope angle (θ)	0, 15, 30, 45, 60, 75 deg
Boundary condition	Top & bottom fixed

$$T(x) = \sqrt{H^2 + V(x)^2} \tag{42}$$

where H, V and x_s are horizontal tension, vertical tension and minimum point which are calculated by

$$H = \frac{wx_L}{\cosh^{-1}\left\{1 - \frac{w^2}{2H^2}(z_L^2 - s_t^2)\right\}} \tag{43}$$

$$V(x) = -H\sinh\left\{\frac{w}{H}(x_s - x)\right\} \tag{44}$$

$$x_s = \frac{H}{w} \ln \frac{w(z_L - s_t)}{H\{\exp(-wx_L/H) - 1} \tag{45}$$

Fig. 4 compares analytic and FEM solutions for curve shape of example catenary in equilibrium position. It is shown that two results agree nearly. Tension distributions of example structure are compared in Fig. 5. They have also good agreements. Analytic horizontal tension, which is constant at any points, is 1,283,528 N. Horizontal tension in FEM is 1,281,571 N. Error is about 0.15 % which shows good accuracy of developed FEM code.

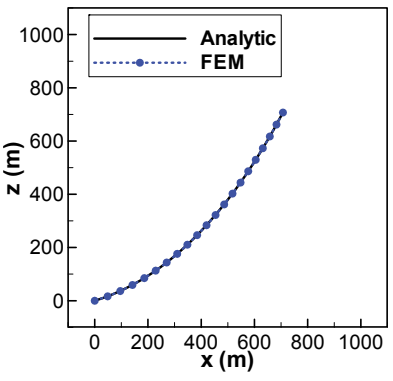

Figure 4: Analytic and FEM results for equilibrium position of example catenary (θ=45 deg)

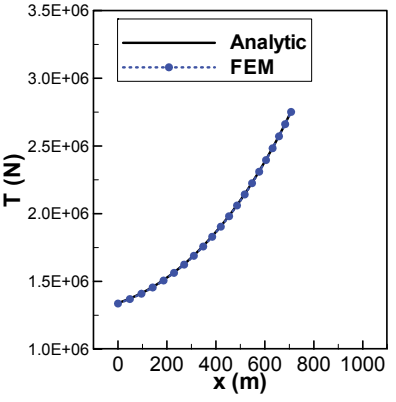

Figure 5: Analytic and FEM results for tension distribution of example catenary (θ=45 deg)

Figs. 6∼17 show curve shape and tension distribution of example catenary structures. It is shown that the smaller axial stiffness, the larger vertical deflection. When the axial stiffness is large, deflection is small. As stiffness increases, the equilibrium position converges to pure catenary curve and the curve shapes are almost identical to those of pure catenary when the non-dimensional stiffness are 100, 300 and 1000. Tensions are generally small when the stiffness is small except tensions near bottom supports of inclined catenaries. As stiffness increases, tension distribution shape converges to that of pure catenary. And, the tension distribution shapes are almost the same as those of pure catnenary when the non-dimensional stiffness are 300 and 1000.

For more quantitative discussion, non-dimensional maximum sags and tensions at top and bottom supports are investigated. Maximum sag versus axial stiffness is plotted in Fig. 18. As stiffness decreases, sag increases because more flexible catenary suffers more axial deformation. As stiffness increases, sag decreases and it

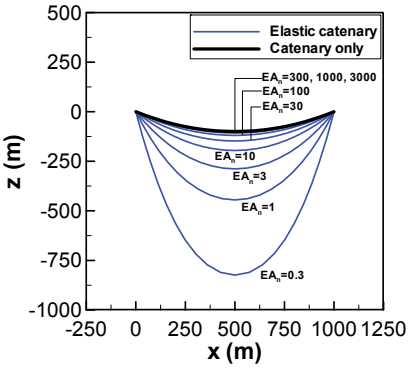

Figure 6: Equilibrium position of example catenary (θ=0 deg)

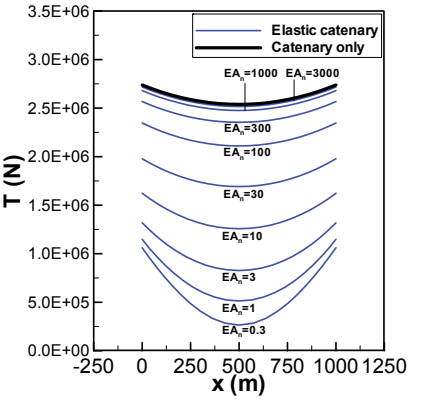

Figure 7: Tension distribution of example catenary (θ=0 deg)

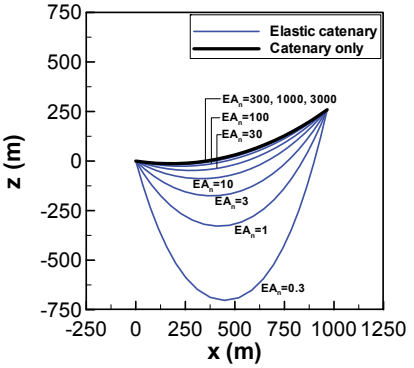

Figure 8: Equilibrium position of example catenary (θ=15 deg)

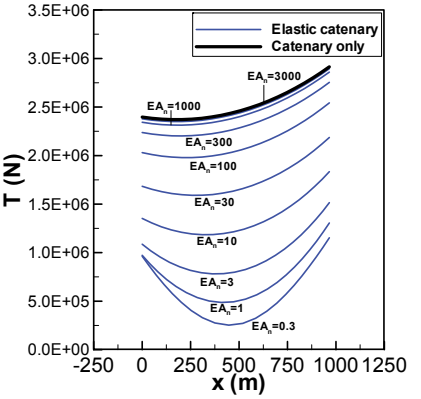

Figure 9: Tension distribution of example catenary (θ=15 deg)

converges asymptotically to that of pure catenary. Figs. 19∼24 show the top and bottom tensions versus axial stiffness. When the catenary is flexible, vertical deflection is large. In that case, tangential angle gets larger at top supports. However, the change of vertical reaction force is relatively small. This induces reduction of horizontal tension resulting in top tension decrease. Therefore, top tension decreases as stiffness decreases. As stiffness increases, top tension increases and it converges asymptotically to that of pure catenary. Bottom tension also decreases as stiffness decrease and vice versa when the catenary is sufficiently stiff. And, it also shows asymptotic behavior. However, when the catenary is flexible, bottom tensions of

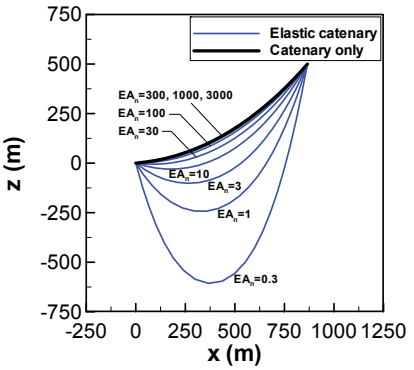

Figure 10: Equilibrium position of example catenary (θ=30 deg)

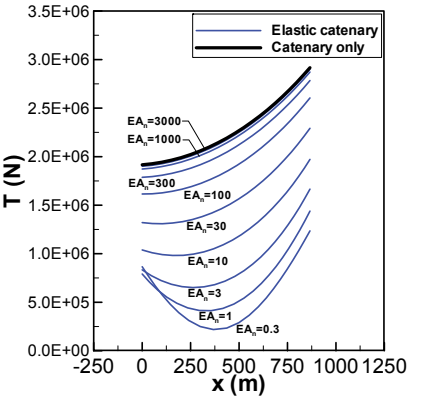

Figure 11: Tension distribution of example catenary (θ=30 deg)

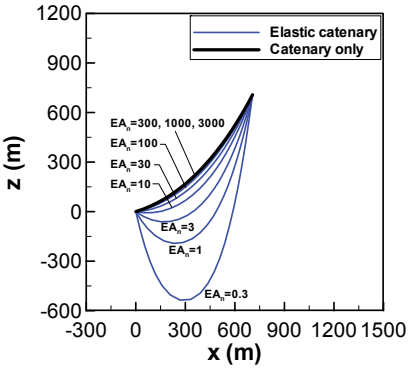

Figure 12: Equilibrium position of example catenary (θ=45 deg)

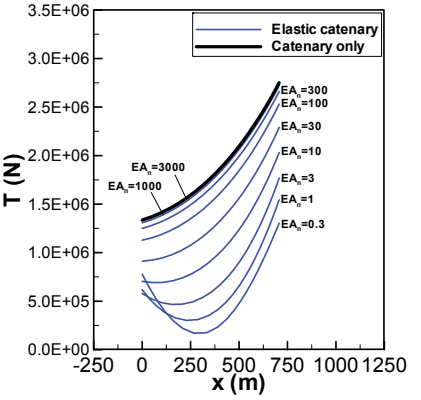

Figure 13: Tension distribution of example catenary (θ=45 deg)

inclined catenary do not show such monotonous increase or decrease. When the catenary gets flexible, gravity center moves left and vertical reaction rapidly becomes large at bottom support. Therefore, bottom tension increases with stiffness decrease in case of inclined flexible catenary. Such tendency is clearer for larger slope angles. If catenary is extremely flexible, tangential lines at top and bottom supports will be almost vertical and tensions will be half of total gravity at both supports. Therefore, normalized tensions at top and bottom supports converge to 0.5 as stiffness decreases.

Results are discussed in point of slope angles of catenary. Fig. 25 shows variation

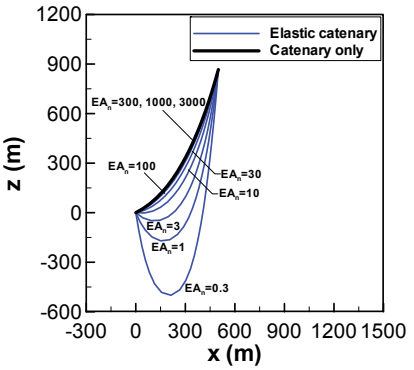

Figure 14: Equilibrium position of example catenary (θ=60 deg)

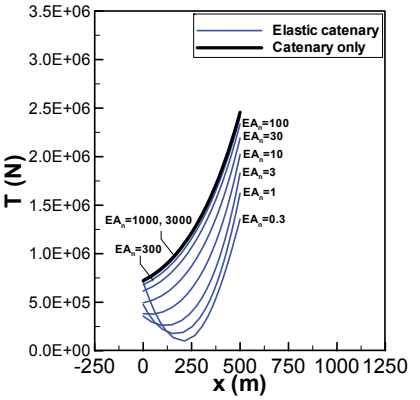

Figure 15: Tension distribution of example catenary (θ=60 deg)

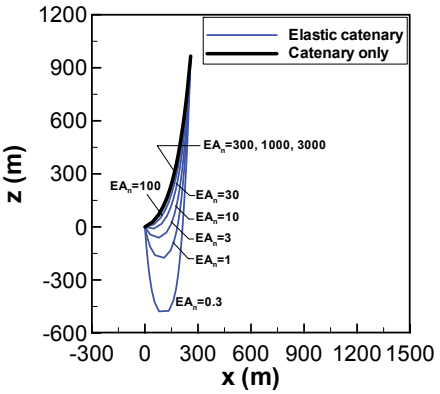

Figure 16: Equilibrium position of example catenary (θ=75 deg)

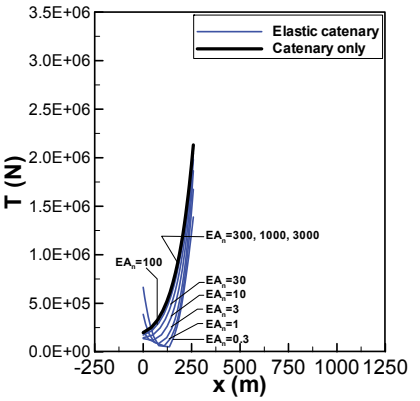

Figure 17: Tension distribution of example catenary (θ=75 deg)

of maximum sag versus slope angle. As slope angle increases, maximum sag increases quadratically. Fig. 26 shows top tension versus slope angles. When the stiffness is large, top tension shows parabolic distribution about slope angles having maximum at 30 or 45 deg. When the stiffness is small, top tension increases slowly with the increase of slope angle. Bottom tension variation versus slope angle is plotted in Fig. 27. It is shown that bottom tension decreases almost linearly as slope angle increases.

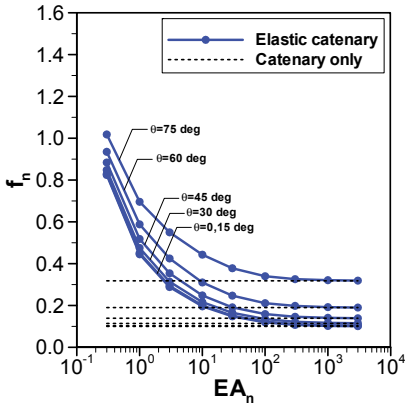

Figure 18: Maximum sag versus axial stiffness

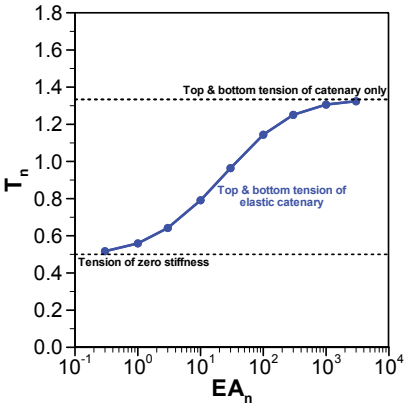

Figure 19: Top and bottom tensions versus axial stiffness (θ=0 deg)

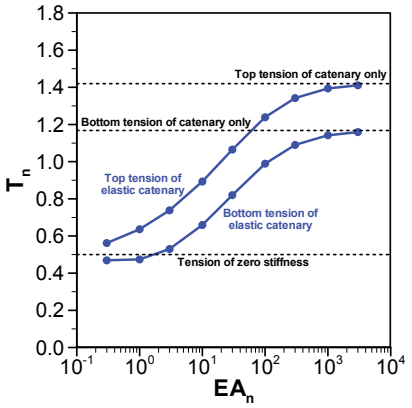

Figure 20: Top and bottom tensions versus axial stiffness (θ=15 deg)

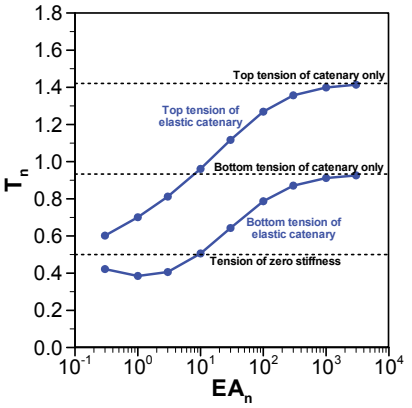

Figure 21: Top and bottom tensions versus axial stiffness (θ=30 deg)

4 Conclusions

In this paper, sag and tension of inclined elastic catenary structure which includes axial deformation as well as pure catenary behavior are investigated with varying axial stiffness and slope angles of catenary. The catenary are analyzed using nonlinear FEM analysis of which numerical code is developed based on minimum potential energy principle and length constraint and verified by comparing with analytic solutions. Some conclusions from parametric analyses are summarized as follows.When the axial stiffness of catenary is smaller, its sag increases because

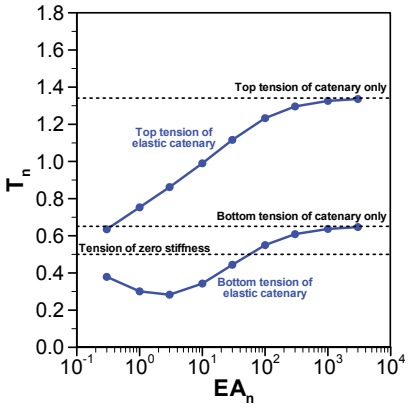

Figure 22: Top and bottom tensions versus axial stiffness (θ=45 deg)

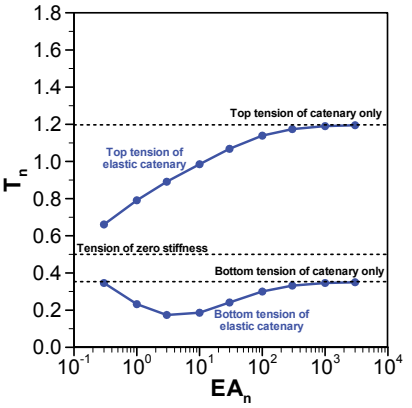

Figure 23: Top and bottom tensions versus axial stiffness (θ=60 deg)

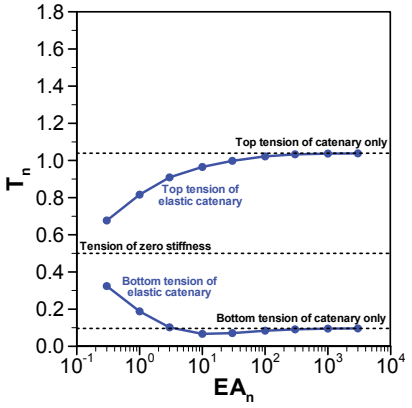

Figure 24: Top and bottom tensions versus axial stiffness (θ=75 deg)

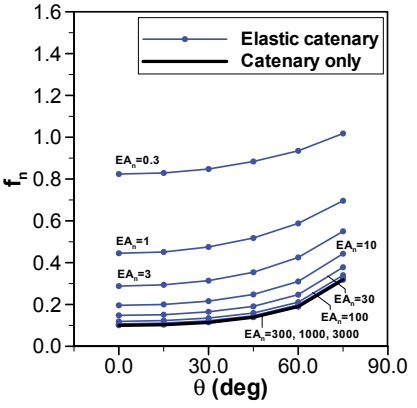

Figure 25: Maximum sag versus slope angle

axial deformation becomes larger. In that case, tangential line is steeper at top support while the variation of vertical components of tension is relatively small. Therefore, horizontal component decreases and total tension also decreases. On the other hand, tension at bottom support becomes larger when the catenary is relatively flexible. This is due to the rapid increase of vertical component of bottom tension by the shift of total gravity center to the left.

When the catenary is very flexible, the magnitudes of both top and bottom tensions converge to half of total gravity because the tangential lines are nearly vertical

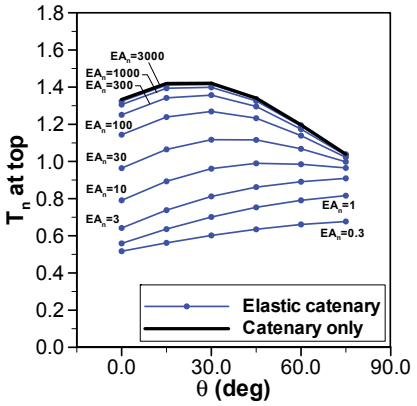

Figure 26: Top tension versus slope angle

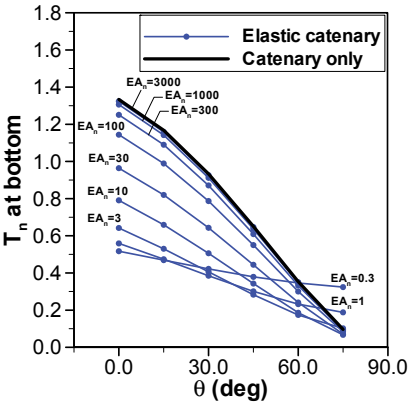

Figure 27: Bottom tension versus slope angle

at both supports. When the catenary is stiffer, the sag decreases and the tension generally increases. And, they asymptotically converge to those of pure catenary.

As slope angle of inclined catenary increases, sag increases quadratically and bottom tension decreases almost linearly. When the catenary is stiff, top tensions are largest at 30 or 45 degree of slope angle. Top tension generally increases for larger slope angle when the catenary is flexible.

Acknowledgement: This study is a part of the project "Development of Engineering Technology of Offshore LNG FSRU" by Ministry of Knowledge Economy of Korea and "Development of Extreme Response Analysis Technologies for Offshore Structures" by Korea Research Council of Fundamental Science & Technology.

References

Arbabi, F. (1991): *Structural Analysis and Behavior*. McGraw-Hill.

Bathe, K. J. (1996): *Finite Element Procedures*. Prentice Hall.

Cui, X. Y.; Liu, G. R.; Li, G. Y.; Zhao, X.; Nguyen, T. T.; Sun, G. Y. (2008): A smoothed finite element method (SFEM) for linear and geometrically nonlinear analysis of plates and shells. *CMES: Computer Modeling in Engineering & Science*, vol. 28, pp. 109–125.

Garrett, D. L. (2005): Coupled analysis of floating production systems. *Ocean Engineering*, vol. 32, pp. 802–816.

Hong, S.; Hong, S. Y. (1997): Effects of mooring line dynamics on position keeping of a floating production system. *Proceeding of the 7th ISOPE Conference*, pp. 336–341.

Irvine, M. (1981): *Cable Structures*. MIT Press.

Okamoto, S.; Omura, Y. (2003): Finite-element nonlinear dynamics of flexible structures in three dimensions. *CMES: Computer Modeling in Engineering & Science*, vol. 4, pp. 287–299.